Abdominal obesity in BTBR male mice is associated with peripheral but not hepatic insulin resistance

Jessica B. Flowers, Angie T. Oler, Samuel T. Nadler, YounJeong Choi, Kathryn L. Schueler, Brian S. Yandell, Christina M. Kendziorski and Alan D. Attie

Am J Physiol Endocrinol Metab 292:936-945, 2007. First published Nov 28, 2006;
doi:10.1152/ajpendo.00370.2006

Am J Physiol Endocrinol Metab 292: E936–E945, 2007.
First published November 28, 2006; doi:10.1152/ajpendo.00370.2006.

Abdominal obesity in BTBR male mice is associated with peripheral but not hepatic insulin resistance

Jessica B. Flowers,[1,2] Angie T. Oler,[2] Samuel T. Nadler,[2] YounJeong Choi,[3] Kathryn L. Schueler,[2] Brian S. Yandell,[3] Christina M. Kendziorski,[4] and Alan D. Attie[2]

Departments of [1]Nutritional Sciences, [2]Biochemistry, [3]Statistics and Horticulture, and [4]Biostatistics and Medical Informatics, University of Wisconsin–Madison, Madison, Wisconsin

Submitted 24 July 2006; accepted in final form 13 November 2006

Flowers JB, Oler AT, Nadler ST, Choi YJ, Schueler KL, Yandell BS, Kendziorski CM, Attie AD. Abdominal obesity in BTBR male mice is associated with peripheral but not hepatic insulin resistance. *Am J Physiol Endocrinol Metab* 292: E936–E945, 2007. First published November 28, 2006; doi:10.1152/ajpendo.00370.2006.—Insulin resistance is a common feature of obesity. BTBR mice have more fat mass than most other inbred mouse strains. On a chow diet, BTBR mice have elevated insulin levels relative to the C57BL/6J (B6) strain. Male F1 progeny of a B6 × BTBR cross are insulin resistant. Previously, we reported insulin resistance in isolated muscle and in isolated adipocytes in this strain. Whereas the muscle insulin resistance was observed only in male F1 mice, adipocyte insulin resistance was also present in male BTBR mice. We examined in vivo mechanisms of insulin resistance with the hyperinsulinemic euglycemic clamp technique. At 10 wk of age, BTBR and F1 mice had a >30% reduction in whole body glucose disposal primarily due to insulin resistance in heart, soleus muscle, and adipose tissue. The increased adipose tissue mass and decreased muscle mass in BTBR and F1 mice were negatively and positively correlated with whole body glucose disposal, respectively. Genes involved in focal adhesion, actin cytoskeleton, and inflammation were more highly expressed in BTBR and F1 than in B6 adipose tissue. The BTBR and F1 mice have higher levels of testosterone, which may be related to the pathological changes in adipose tissue that lead to systemic insulin resistance. Despite profound peripheral insulin resistance, BTBR and F1 mice retained hepatic insulin sensitivity. These studies reveal a genetic difference in body composition that correlates with large differences in peripheral insulin sensitivity.

mouse genetics; adipose; insulin sensitivity

INSULIN RESISTANCE IS A PREDIABETIC SYNDROME (8, 49, 63, 74). Over 40 million Americans are estimated to be insulin resistant (3). Not all individuals with impaired insulin sensitivity will go on to develop type 2 diabetes; however, increased morbidity and mortality already exist in insulin-resistant individuals (23, 29, 38, 39).

The distribution of excess fat may be the most important determinant of overall risk for complications of insulin resistance such as cardiovascular disease (67). The body mass index is widely used for assessing risk of insulin resistance and its common comorbidities (2, 18) but fails to account for individuals who are heavy due to muscularity or those who have a normal body weight but still have excess abdominal adiposity. Excess abdominal fat is associated with a much greater risk of morbidity and mortality than is excess subcutaneous fat (60, 69, 79). It is estimated that 13–18% of individuals with normal body mass index have significant risk factors for diabetes and cardiovascular disease (17, 42). Factors such as sex and race appear to influence fat distribution and also the threshold for which excess adipose tissue results in insulin resistance and cardiovascular complications (19, 30, 52, 53, 56). The mechanisms linking fat localization and pathogenicity remain poorly understood. Finding models to adequately represent the spectrum of weight distribution and associated risks will help us to understand this complex process.

Inbred mouse strains replicate much of the genetic and sex variation in human insulin sensitivity. We have focused on the BTBR strain, which replicates many features of insulin resistance found in humans with excess visceral adiposity. Leptin-deficient BTBR *ob/ob* mice are a particularly useful animal model for studying obesity-related diabetes. Unlike the B6 *leptin*$^{ob/ob}$ mice, which develop only a moderate hyperglycemia, BTBR *leptin*$^{ob/ob}$ mice become severely diabetic (73). Human studies have demonstrated that, prior to the onset of hyperglycemia, insulin resistance is an important predictor of diabetes susceptibility in relatives of type 2 diabetics (26, 28, 31). Therefore, by examining differences between BTBR and B6 lean mice, we may determine specific factors that confer increased diabetes susceptibility prior to the onset of disease.

Our laboratory has found that, even in the absence of the obesity imposed by leptin deficiency, BTBR mice have elevated insulin levels relative to the B6 mouse strain (73). Male F1 progeny of a B6 × BTBR cross (F1) have increased abdominal obesity, hyperinsulinemia, hypertriglyceridemia, and hypercholesterolemia (65). These phenotypes are present in association with impaired glucose tolerance and reduced insulin-stimulated glucose uptake into isolated muscles (65). Further characterization of the insulin-resistant phenotype of F1 male mice revealed a blunted insulin response in isolated adipocytes (57). Adipocyte insulin resistance is also present in BTBR males (12). In contrast, muscle insulin resistance was observed only in F1 males (65). Consistent with other studies demonstrating protection from insulin resistance and diabetes in female rodents (34, 47, 51), neither adipocyte nor muscle insulin resistance was observed in female mice of either strain (12, 57, 65).

Tissue-specific deletion of the GLUT4 glucose transporter or the insulin receptor has revealed that defects in individual tissues can have systemic consequences (54). Most surprising was the finding that loss of glucose sensing in adipose tissue could result in insulin resistance in muscle (1). We hypothe-

Address for reprint requests and other correspondence: A. D. Attie, Dept. of Biochemistry, Univ. of Wisconsin–Madison, 433 Babcock Dr., Madison, WI 53706 (e-mail: attie@biochem.wisc.edu).

The costs of publication of this article were defrayed in part by the payment of page charges. The article must therefore be hereby marked "*advertisement*" in accordance with 18 U.S.C. Section 1734 solely to indicate this fact.

sized that muscle insulin resistance in BTBR mice may be revealed by in vivo studies of insulin sensitivity.

To determine the interplay among tissues contributing to insulin resistance in our model, we performed hyperinsulinemic euglycemic clamp experiments. We determined that BTBR and F1 mice exhibit insulin resistance primarily in heart, soleus muscle, and adipose tissue. In contrast, the liver showed normal insulin sensitivity. Thus, BTBR and F1 male mice present a model of abdominal obesity associated with peripheral but not hepatic insulin resistance.

METHODS

Animals. BTBR T+ tf/J (BTBR) and C57BL/6J (B6) animals were purchased from the Jackson Laboratory (Bar Harbor, ME) and bred at the University of Wisconsin–Madison. F1 mice were generated by breeding a B6 male to a BTBR female. Mice were housed on a 12:12-h light-dark cycle, lights on at 0600. Mice had free access to a chow diet of roughly 6% fat (by mass, Purina 5008) and water, except for during fasts and during the clamp procedure. Research protocols were approved by the University of Wisconsin Institutional Animal Care and Use Committee.

Surgery. Four to six days prior to the clamp, mice were catheterized through the right jugular vein. Surgeries were carried out under isoflurane anesthesia. A Silastic catheter (0.025 in. OD; VWR International, West Chester, PA) filled with saline was inserted via a right lateral neck incision, advanced into the superior vena cava via the right internal jugular vein, and sutured in place. The catheter was then knotted at the distal end, tunneled subcutaneously, exteriorized at the dorsal cervical midline, and then further tunneled subcutaneously. A silk suture was fastened around the catheter at the neck site. On the day of the clamp, the catheter was externalized by pulling the suture through the dorsal cervical incision site.

Hyperinsulinemic euglycemic clamp. Mice were brought to the experimental room and fasted at 1000. At 1330, basal mice were placed in broom-style restrainers, and catheters were externalized. Tails were anesthetized with lidocaine and prilocaine cream (2.5%/2.5%; E. Fougera, Atlanta, Melville, NY), and mice were allowed to acclimate to their confinement. At 1400, the tail was clipped, and the catheter was connected to a pump (model 102; CMA Micodialysis, Solna, Sweden). HPLC-purified [3-^{3}H]glucose (PerkinElmer Life Sciences, Boston, MA) was infused at 0.055 uCi/min in saline at a rate of 3.3 μl/min. Blood (30 μl) was collected by gently massaging the tail at 90, 100, and 110 min for determination of blood glucose and plasma specific activity. At 1530, clamp mice were placed in broom-style restrainers and catheters were externalized. Tails were anesthetized, and mice were allowed to acclimate to their confinement. At 1600, the tail was clipped, and the catheter was connected to a pump. A saline solution was infused at 3.3 μl/min containing human insulin (2.5 mU·kg^{-1}·min^{-1} Humulin R; Eli Lilly, Indianapolis, IN) along with [3-^{3}H]glucose (0.1,375 μCi/min; PerkinElmer Life Sciences) and 2-deoxy-D-[1-^{14}C]glucose (0.825 μCi/min; PerkinElmer Life Sciences) for the determination of whole body glucose fluxes and tissue glucose uptake, respectively. Dextrose solution (20%; Phoenix Pharmaceuticals, St. Joseph, MO) was infused at a variable rate to maintain blood glucose at ~100 mg/dl. Blood (~8 μl) was collected initially and every 10 min throughout the 2-h infusion for determination of glucose concentration. Additional blood (20 μl) was collected at 70, 80, 90, 100, 110, and 120 min for determination of specific activity. Following the last tail bleed, mice were disconnected from the pump and killed with an isoflurane overdose. Following respiratory arrest, a heart puncture was performed for blood collection and heart, liver, epididymal white adipose tissue (EpiWAT), soleus muscle, and quadriceps muscle were removed and immediately frozen in liquid nitrogen and then transferred to a −80°C freezer.

Assays. Glucose concentration was analyzed using a hand-held glucose monitor (Prestige IQ; Home Diagnostics, Fort Lauderdale, FL). Plasma glucose was estimated as blood glucose multiplied by 1.12 as referenced by the glucometer manufacturer (Home Diagnostics). Plasma insulin concentrations were measured by radioimmunoassay kit (Linco Research, St. Charles, MO). Plasma testosterone levels were measured using the DSL-4000 ACTIVE testosterone radioimmunoassay kit (Diagnostic Systems Laboratories, Webster, TX). Plasma concentrations of [3-^{3}H]glucose, 2-deoxy-D-[1-^{14}C]glucose (2-DG), and [^{3}H]H_2O were determined after deproteinization of plasma samples with $Ba(OH)_2$ and Zn_2SO_4, as previously described (45). For the determination of tissue 2-deoxy-D-[1-^{14}C]glucose-6-phosphate (2-DG-6-*P*) content, tissues were homogenized, and the supernatants were subjected to an ion exchange column (Poly-Prep 731–6211; Bio-Rad Laboratories, Hercules, CA) to separate 2-DG-6-*P* from 2-DG (45). ^{3}H and ^{14}C were counted in Bio-Safe II scintillation fluid (Research Products, Mount Prospect, IL) on a scintillation counter (PerkinElmer, Shelton, CT).

Calculations. Basal hepatic glucose output was calculated as the ratio of the [3-^{3}H]glucose infusion rate (dpm/min) to the specific activity of plasma glucose (dpm/mg) at 90, 100, and 110 min. Clamp whole body glucose uptake was calculated as the ratio of [3-^{3}H]glucose infusion rate (dpm/min) to the specific activity of plasma glucose (mean of the 90- to 120-min samples). Because ^{3}H on the C-3 position of glucose is lost to water during glycolysis, the rate of glycolysis can be determined from the rate of increase in plasma [^{3}H]H_2O determined by linear regression using the 70- to 120-min points (66). Plasma [^{3}H]H_2O was calculated as the difference between nondried and dried plasma ^{3}H counts. Plasma was dried under nitrogen gas. For calculating the rate of whole body glycolysis, the body was assumed to be 65% and the plasma 93% water (66). Clamp hepatic glucose output was determined by subtracting the average steady-state glucose infusion rate in the last 40 min of the clamp from the whole body glucose uptake (45). The rate of whole body glycogen synthesis was estimated by subtracting the rate of glycolysis from whole body glucose disposal (66). Muscle and white adipose tissue glucose uptake were calculated from the average plasma 2-DG specific activity (70- to 120-min points) and tissue 2-DG-6-*P* content. All measurements were made when steady-state conditions were achieved.

Real-time quantitative PCR. RNA was isolated from individual livers by use of RNeasy minicolumns with on-column DNase digestion (Qiagen, Valencia, CA). First-strand cDNA was synthesized from 1 μg of total liver RNA, or 0.3 μg of adipose tissue RNA using SuperScript III Reverse Transcriptase primed with a mixture of oligo(dT) and random hexamers (Invitrogen Life Sciences, Carlsbad, CA). Reactions lacking the reverse transcriptase served as control for amplification of genomic DNA. Liver reactions were performed on an ABI GeneAmp 5700 Sequence Detection System (Applied Biosystems, Foster City, CA) and carried out in a 25-μl volume of 1× SYBR Green PCR Core Reagents (Sigma-Aldrich, St. Louis, MO) containing cDNA template from 10 ng of total RNA and 6 pmol primers. Adipose tissue reactions were performed on an ABI GeneAmp 7500 Sequence Detection System (Applied Biosystems) and carried out in a 20-μl volume of 1× ABI SYBR Green PCR Master Mix containing cDNA template from 3 ng of total RNA and 6 pmol primers. We determined the cycle at which the abundance of the accumulated PCR product crossed a specific threshold, the threshold cycle (C_T), for each reaction. For hepatic measurements, differences in C_T values between β-actin (M12481) and phospho*enol*pyruvate carboxykinase (PEPCK; NM_011044) or G-6-Pase (NM_008061) were calculated for each individual, and in the adipose tissue acidic ribosomal phosphoprotein P0 (Arbp; NM_007475) was used as a normalization control. Gene-specific primers were designed for standard RT-PCR cycling parameters using Primer Express software v. 1.0–2.0 (Applied Biosystems). Specificity was determined by observation of a single dissociation peak and by aligning primers in the University of California-Santa Cruz Mouse Genome Browser (genome.ucsc.edu, February 2006

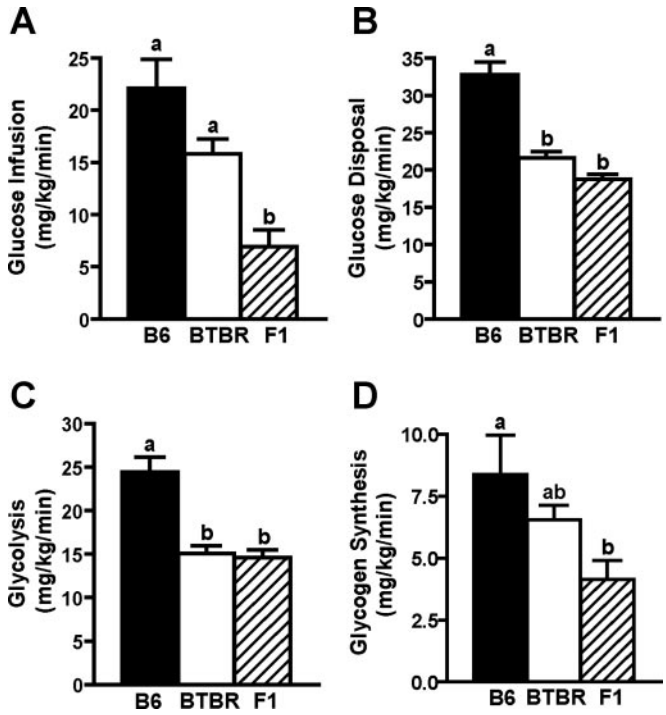

Fig. 1. In vivo whole body glucose flux during hyperinsulinemic euglycemic clamp studies in awake, male mice at 10 wk of age. *A*: glucose infusion. *B*: whole body glucose disposal. *C*: glycolysis. *D*: glycogen synthesis. Data represent means ± SE of 6–7 mice per group. Different letters designate a statistically significant difference by one-way ANOVA with Tukey post test, $P < 0.05$.

version). We were unable to develop isoform-specific RT-PCR primers for Pir isoforms (designated Pir.s), given their high homology. Accession numbers for the genes analyzed are given in Table 2.

Microarray data analysis. To examine the changes in gene expression among lean groups of animals, we chose to reanalyze murine 11K microarray data previously obtained by our laboratory (data available through NCBI GEO; GSE2952). As described previously, epididymal fat pads were isolated from 14-wk-old mice after a 4-h fast (58). RNA was isolated and cDNA prepared from equal amounts of RNA pooled from at least four animals. In the new analysis, quantitative expression levels of all the transcripts were preprocessed using the robust multiarray average (RMA) algorithm for normalization (40). Expression measurements were analyzed, and statistically significant differential expression was determined using the empirical Bayes methodology EBarrays (43, 59), which are implemented in *R*, a publicly available statistical analysis environment (75). For each comparison, we identified a list of differentially expressed transcripts with false discovery rate (FDR) at 5%.

Statistics. All data are represented as means ± SE. Comparisons among three groups were made using one-way ANOVA, and when significance was observed, post hoc Tukey tests were performed using GraphPad Prism v. 4.02 for Windows (GraphPad Software, San Diego, CA). Comparisons of two groups were done using an unpaired Student's *t*-test in GraphPad or Microsoft Excel (© 2002). Regression analyses were performed in Systat v. 8.0 (SPSS). Heat plots of regression coefficients were generated in *R* (75). Statistical significance was set at $P < 0.05$.

RESULTS

Whole body glucose metabolism. To determine the effects of strain background on whole body glucose metabolism, we performed hyperinsulinemic euglycemic clamp experiments. Because the B6 strain has a lower basal insulin level than the BTBR or the F1 mice, we chose to expose the three groups of mice to the same amount of insulin to measure the response to an equal insulin dose rather than try to achieve the same steady-state insulin level. Indeed, the insulin infusion raised insulin levels by about the same amount in all three mouse groups. The alternative would have been to match all three groups for the steady-state insulin level. This would have required us to deliver a different amount of insulin to the B6 mice than to the other two groups.

The rate of glucose infusion needed to maintain euglycemia at ~100 mg/dl was highest in B6 mice, tended to be lower in BTBR mice ($P = 0.12$), and was significantly lower in F1 mice than in either parental strain (22.1 ± 2.8 and 15.8 ± 1.4 vs. 6.9 ± 1.6 mg·kg^{-1}·min^{-1}, $P < 0.001$ and $P < 0.05$, respectively; Fig. 1*A*). Compared with B6 mice, glucose disposal in BTBR and F1 mice was reduced by 34 and 43%, respectively (Fig. 1*B*). Two processes contribute to glucose disposal: glycogen synthesis and glycolysis. Glycolysis, which accounted for the majority of glucose disposal, was reduced by 40% in BTBR and F1 mice (Fig. 1*C*). Glycogen synthesis was slightly lower in BTBR mice and was significantly lower in F1 mice than in B6 mice (Fig. 1*D*). Thus, BTBR and F1 mice have significantly reduced glucose disposal, primarily due to a defect in glycolysis.

Body composition effects on glucose metabolism. Despite reduced body weight, B6 mice disposed of ~20% more total glucose than either BTBR or F1 mice. To determine the tissues responsible for the decreased whole body glucose disposal in BTBR and F1 mice, we measured the rate of 2-DG uptake in individual tissues. Insulin-stimulated glucose uptake in heart was decreased by over 50% in BTBR and F1 mice (Fig. 2*A*). Glucose uptake in soleus muscle was reduced by 56% in BTBR and 72% in F1 mice, respectively (Fig. 2*B*). Insulin resistance in the heart and soleus muscles, which are composed mainly of red or oxidative muscle fibers, is consistent with previous work demonstrating that red muscle fibers are more susceptible to insulin resistance than white muscle fibers (10, 22, 32, 33). The quadriceps muscle is primarily composed of white muscle fibers but does contain red muscle fibers. In contrast to heart and soleus muscle, quadriceps muscle glucose uptake was increased approximately twofold in BTBR compared with B6 and F1 mice (Fig. 2*C*). The increase in glucose uptake in quadriceps muscle of BTBR mice suggests altered quadriceps muscle fiber composition or compensation for reduced disposal in the more oxidative heart and soleus muscles.

Fig. 2. Correlation among body composition factors and whole body glucose disposal (GDISP). Tissue specific 2-deoxyglucose disposal in heart muscle (*A*), soleus muscle (*B*), quadriceps muscle (*C*), and epididymal white adipose tissue (EpiWAT; *D*). Data represent means ± SE of 4–7 mice per group. Different letters designate a statistically significant difference by one-way ANOVA with Tukey's post test. *E*: tissue mass normalized to body weight and expressed relative to B6 mice. *F*: product of rate of tissue glucose uptake and tissue mass expressed relative to the 4-tissue total for B6 mice. *G*: body weight in grams (BW), white adipose tissue %BW (WAT), quadriceps muscle %BW (QUAD), and soleus muscle %BW show significant correlations with each other and with GDISP. Scatter plots of data are illustrated at *bottom left* of the graph with individual measures shown for B6 (●), BTBR (○), and F1 (hatched circles). Diagonal illustrates that the data are normally distributed for each genotype. *Right*: Pearson correlation coefficients for each comparison, $P < 0.05$.

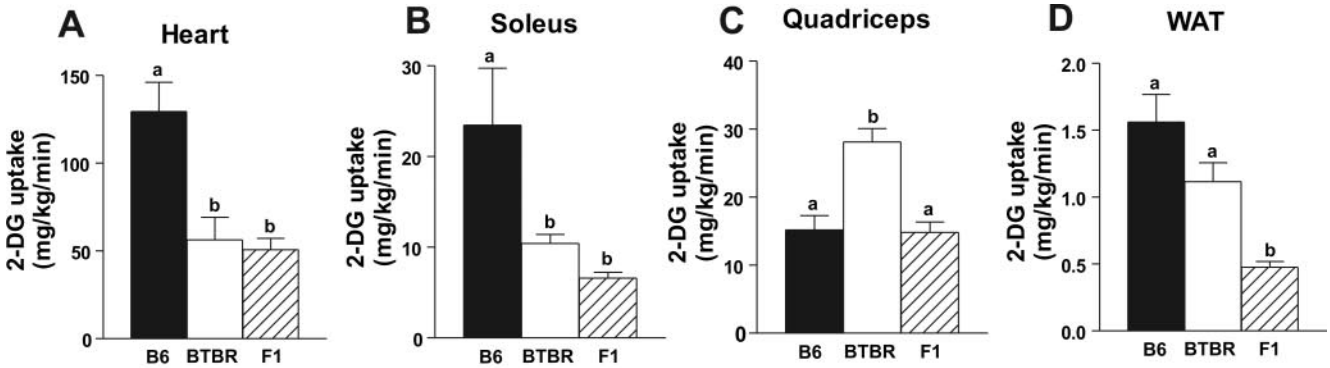

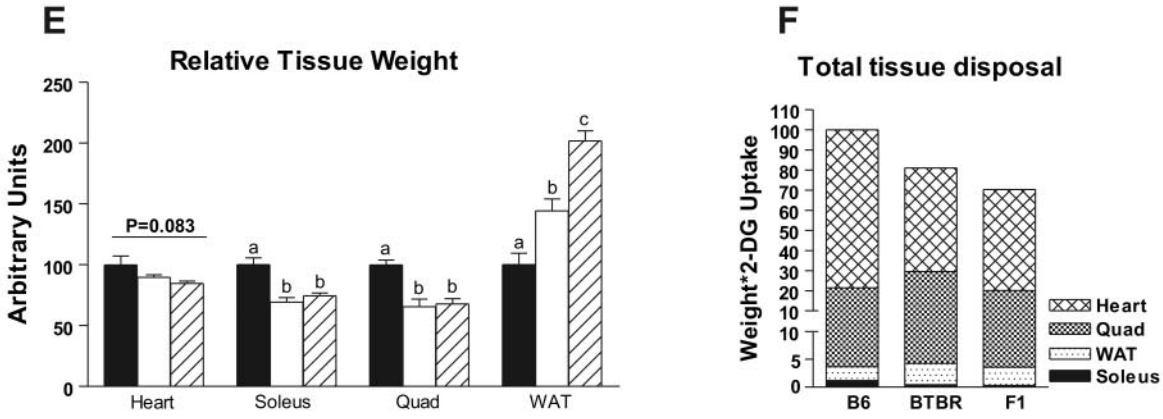

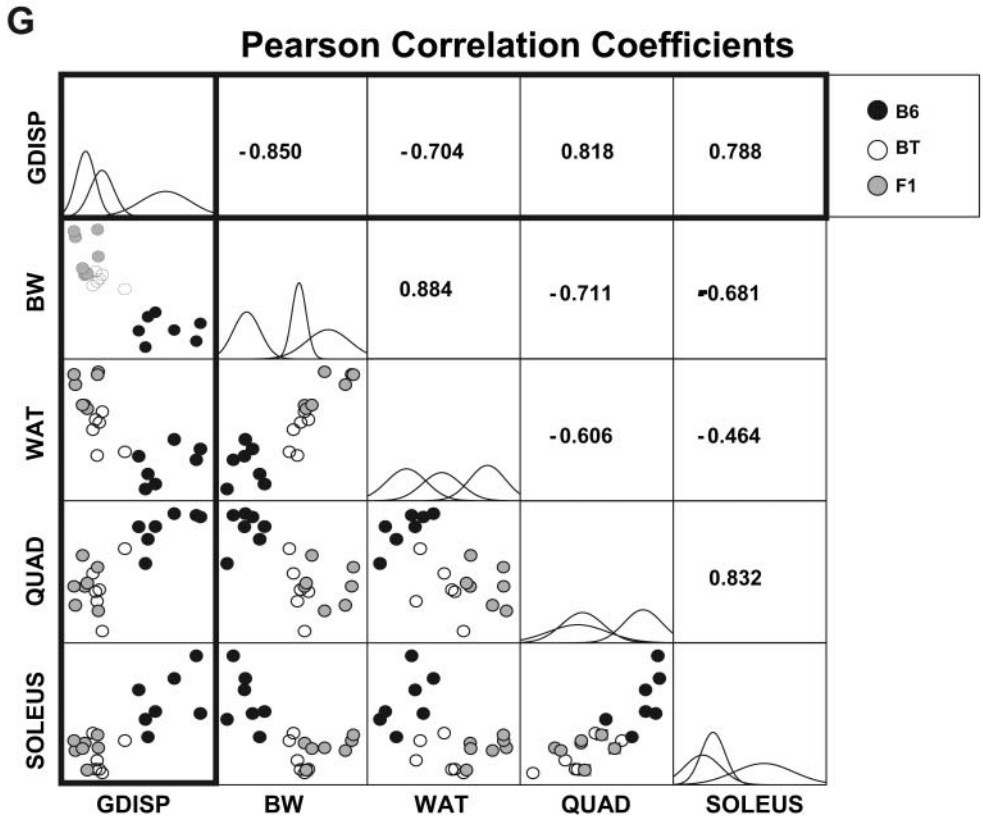

In WAT, glucose uptake was slightly reduced in BTBR mice but reduced by 58% in F1 mice (Fig. 2*D*). Although our previous reports noted profound insulin resistance in isolated adipocytes (12, 57), these results demonstrate that, when in direct competition with more metabolically active tissues, adipose tissue differences are dampened.

In addition to altered glucose uptake in various tissues, we observed strain differences in tissue mass. Relative to B6 mice, BTBR and F1 mice had a 50 and 100% increase, respectively, in EpiWAT mass and, surprisingly, a 30% decrease in quadriceps and soleus muscle mass (Table 1 and Fig. 2*E*). To fully assess the contribution of each tissue to total glucose disposal, we calculated the product of the tissue mass and the 2-DG uptake measurement. With this calculation, we have almost completely captured the strain differences in whole body glucose disposal, with BTBR having ~80% and F1 70% of the B6 glucose disposal by four tissues (Fig. 2*F*). The increased adipose mass in BTBR and F1 mice compensates for reduced adipose glucose disposal but is insufficient to overcome the differences in muscle mass and glucose disposal. Although quadriceps and soleus muscle mass was positively correlated with whole body glucose disposal (GDISP), body weight and WAT mass were negatively correlated with GDISP (Table 1 and Fig. 2*G*). Heart and liver mass did not show a correlation with GDISP. These correlation trends were similar for rates of glycolysis and glycogen synthesis (Table 1). Therefore, increased adipose tissue can predict reduced glucose disposal, whereas increased muscle can predict enhanced glucose disposal.

Adipose tissue gene expression. Insulin resistance originating in adipose tissue may affect all insulin target tissues (1). Muscle insulin resistance in BTBR mice was observed only in vivo, whereas adipose tissue has in vitro differences in insulin sensitivity, suggesting that the defect in adipose tissue is a primary effect and the muscle changes might be secondary.

We were interested in identifying the transcripts whose abundance changed with modest differences in adiposity and insulin sensitivity. We (58) previously reported on adipose tissue transcripts whose abundance changed in mice when they became severely obese with the *leptin*$^{ob/ob}$ mutation. Thus, we reanalyzed our data and identified changes in lean male mice. After RMA normalization of the data, we used the EBarrays algorithm to identify genes that were differently expressed. Using the KEGG and Biocarta pathway tools, available through Web-based Gene Set Analysis Toolkit (85) (bioinfo.vanderbilt.edu/webgestalt), we selected genes with known pathway enrichment and confirmed these by RT-PCR using adipose tissue cDNA from animals subjected to the clamp procedure. We confirmed 15 genes as being significantly differentially expressed (Table 2). Five additional genes that were predicted to be decreased in B6 (*Cck, Cebpb, Egf, Ifitm3, Pla2g12a)* and four that were predicted to be increased (*Akr1b7, Cd52, Il2ra, Tnfrsf8)* were tested but not confirmed. It is possible that these genes may be false positives. However, with ~100 genes predicted to be different, we would expect, at most, five genes to be false positives. A more plausible explanation is that some of these genes may be differentially regulated during fasting vs. clamp conditions.

Several of the differentially expressed genes are related to cytoskeletal structure and function (*Acta, Actb, Diap1, Rhoa*). Insulin signaling induces cytoskeletal changes that are necessary for GLUT4 movement to the cell surface (27, 77). Cytoskeletal changes also occur to accommodate the expansion of adipocytes (70, 71). Increased *leptin* gene expression in BTBR and F1 mice is a good indicator of enlarged adipocytes (20, 50).

Filamin (*Flna*) as well as several of the cytoskeletal genes (*Actb, Diap1, Rhoa*) are involved in focal adhesion. Formation of focal adhesions and remodeling of actin are important steps in adipocyte hyperplasia (6). Focal adhesions are cell membrane structures that contain several signaling molecules involved in the regulation of cell growth, including mitogen-activated protein kinases (MAPK) (68).

Control of signaling through MAPK pathways or the insulin-signaling pathway occurs through a series of phosphorylation-dephosphorylation events. Whereas altered phosphorylation of MAPK pathway components can affect proliferation of adipose tissue, phosphorylation of the insulin receptor regulates insulin sensitivity. Consistent with the microarray results, we found three phosphatases (*Ppp2r4*, *Ppp6c*, and *Ptprs*) to be upregulated in BTBR and F1 mice (Table 2). Although these phosphatases do not have a known role in adipose tissue, their impacts on intracellular signaling warrant further investigation, as their expression levels were highly negatively correlated with whole body glucose disposal (Table 2 and Fig. 3).

Increased adiposity has previously been associated with increased inflammation (64, 80, 81, 83). Consistent with increased inflammation in adipose tissue from BTBR and F1 mice, several genes involved in inflammatory pathways were differentially expressed [*Cflar, Fos, H2ab1,* Pir.s *(Pira6a, Pira6b, and Pirb/Lilrb), Ptgs2,* and *Syk*]. In addition to promoting insulin resistance (35, 36, 62, 78), inflammatory factors can affect muscle mass by inhibiting de novo protein synthesis or by promoting muscle breakdown (11, 48). This predicts that adipose tissue expression of inflammatory genes would be

Table 1. *Body composition and correlation with glucose metabolism*

	B6	BTBR	F1	GDISP	Glycolysis	Glycogen
Body weight, g	26.3±0.6*	32.8±0.4†	36.5±1.0^{c}	−0.850	−0.749	−0.511
Liver, %BW	3.8±0.08	3.90±0.23	3.70±0.05	NS	NS	NS
EpiWAT, %BW	1.26±0.12*	1.82±0.13†	2.55±0.11^{c}	−0.704	−0.504	−0.623
Quadriceps, %BW	0.685±0.018*	0.448±0.023†	0.465±0.029†	0.818	0.677	0.567
Heart, %BW	0.507±0.037	0.455±0.010	0.430±0.009	NS	NS	0.511
Soleus, %BW	0.029±0.002*	0.020±0.001†	0.022±0.001†	0.788	0.789	NS

Values are means ± SE of 6–7 mice per group. Tissue weights are from 10-wk-old male mice and are normalized to body weight (BW). Different symbols designate a statistically significant difference by one-way ANOVA with Tukey's post test, $P < 0.05$. Nos. sharing the same symbols are not significantly different. Pearson correlation coefficients for significant correlations ($P < 0.05$) are shown for whole body glucose disposal (GDISP), rate of glycolysis, and rate of glycogen synthesis.

Table 2. *Gene expression changes in adipose tissue correlated with glucose disposal, muscle mass, and testosterone*

Accession No.	Symbol	Description	Fold	*P* Value	GDISP Corr	*P* Value	Quad Corr	*P* Value	Sol Corr	*P* Value	Testosterone	*P* Value
					Cytoskeletal and focal adhesion***							
M12481	Actb*,**	Actin, beta, cytoplasmic	5.4	0.000	−0.850	0.000	−0.850	0.000	−0.807	0.000	0.588	0.007
BC064800	Acta2*	Actin, alpha 2, smooth muscle, aorta	2.7	0.001	−0.675	0.001	−0.782	0.000	−0.618	0.002	0.369	0.109
XM_289920	Flna**	Filamin, alpha	2.2	0.006	−0.627	0.003	−0.700	0.001	−0.679	0.000	0.279	0.233
NM_007858	Diap1*,**	Diaphanous homolog 1 (Drosophila)	2.2	0.000	−0.741	0.000	−0.710	0.000	−0.650	0.002	0.577	0.008
NM_016802	Rhoa*,**	Ras homolog gene family, member A	1.7	0.002	−0.614	0.004	−0.342	0.140	−0.428	0.059	0.305	0.191
					Inflammation							
***	Pir's	Paired-lg-like receptors (Pira6-a & -b isoforms, Lilrb3/Pirb)	6.6	0.001	−0.744	0.000	−0.860	0.000	−0.785	0.000	0.651	0.002
NM_010234	Fos	FBJ osteosarcoma oncogene	4.2	0.027	−0.340	0.143	−0.376	0.103	−0.342	0.182	0.388	0.091
M64291	Ptgs2	Prostaglandin-endoperoxide synthase 2	2.7	0.039	−0.436	0.062	−0.512	0.025	−0.514	0.024	0.522	0.022
NM_011518	Syk	Spleen tyrosine kinase	2.5	0.005	−0.574	0.008	−0.715	0.000	−0.624	0.003	0.630	0.003
NM_207653	Cflar	CASP8 and FADD-like apoptosis regulator	1.9	0.001	−0.730	0.000	−0.647	0.003	−0.610	0.001	0.587	0.008
NM_010379	H2ab1	Histocompatibility 2, class II antigen A, beta 1	1.5	0.013	−0.412	0.071	−0.339	0.143	−0.312	0.120	0.491	0.028
					Phosphatase							
NM_011218	Ptprs	Protein tyrosine phosphatase	4.5	0.000	−0.832	0.000	−0.839	0.000	−0.843	0.000	0.589	0.006
NM_138748	Ppp2r4	Protein phosphatase 2A, regulatory subunit B (PR53)	1.7	0.001	−0.701	0.001	−0.662	0.002	−0.651	0.000	0.510	0.022
NM_024209	Ppp6c	Protein phosphatase 6, catalytic subunit	1.5	0.003	−0.689	0.001	−0.650	0.002	−0.710	0.001	0.390	0.089
					Adipokine							
U18812	Lep	Leptin	6.2	0.000	−0.852	0.000	−0.779	0.000	−0.730	0.000	0.519	0.269

Expression measurements were determined for 6–7 mice per genotype. Individual values were normalized to *Arbp* and then expressed relative to B6 mice. Fold change represents the average of BTBR and F1 animals. Corr, Pearson correlations between individual expression values and GDISP; quadriceps muscle (Quad), soleus muscle (Sol), and plasma testosterone values. ***NM_008848, NM_011093, NM_011095.

negatively correlated with muscle mass. As indicated in Table 2 and Fig. 3, gene expression changes in adipose tissue were negatively correlated with muscle weight.

Testosterone and insulin resistance. Determining whether hyperandrogenemia promotes or protects against insulin resistance has been a complicated issue. Whereas hyperandrogenemia and insulin resistance are common features of polycystic ovary syndrome (16, 61), hypoandrogenemia has also been associated with increased insulin resistance in men (41, 61). Whether hyperandrogenemia is the cause or the consequence of insulin resistance remains undetermined. Testosterone could directly induce insulin resistance by inhibiting secretion of adiponectin (82). However, there is also evidence suggesting that hyperinsulinemia drives androgen production (5). Irrespective of the cause, higher testosterone levels could drive inflammation (4, 25). Given that adipocyte and muscle insulin resistance was observed only in male mice, we determined whether these defects were related to differences in testosterone levels. Testosterone levels tended to be higher in F1 mice and were significantly higher in BTBR mice compared with B6 mice (0.41 ± 0.04 and 0.46 ± 0.05 vs. 0.28 ± 0.04 ng/ml, $P = 0.14$ and $P = 0.04$, respectively). Consistent with induced androgen signaling (24), there was a significant positive correlation between plasma testosterone concentration and Cflar/c-FLIP mRNA expression ($R = 0.587$, $P = 0.008$; Table 2). Testosterone levels were also positively correlated with other differentially expressed genes and negatively correlated with whole body glucose disposal (Table 2 and Fig. 3).

Plasma chemistry and hepatic insulin sensitivity. During the clamp experiments, we infused insulin to measure the responsiveness of the liver. Despite whole body insulin resistance, BTBR and F1 mice exhibited normal hepatic insulin sensitivity. This was illustrated by a greater than 50% reduction in hepatic glucose output (HGO) under conditions of physiological hyperinsulinemia (Fig. 4*A*). Somewhat surprisingly, B6 mice exhibited higher basal/fasting HGO than BTBR or F1 mice (Fig. 4*A*). However, fasting plasma insulin was ~80% lower in B6 mice (Table 3). Therefore, this seemingly predi-

abetic hyperglycemic phenotype seen in B6 mice is likely due to the differences in fasting insulin. Insulin secretion defects in B6 mice have been reported (76) and are predominantly due to a mutation in nicotinamide nucleotide transhydrogenase (21). Following insulin infusion, when insulin levels were similarly raised in all groups by ~0.5 ng/ml (Table 3), HGO was not different among the strains of mice (Fig. 4*A*), a result indicating that the fasting hyperglycemia observed in B6 mice was not due to hepatic insulin resistance.

As a further assessment of hepatic insulin sensitivity, we measured the expression of gluconeogenic enzymes, *PEPCK* and *G6Pase*. PEPCK and G6Pase are regulated at the transcriptional level by insulin and are important determinants of hepatic glucose output. We determined that expression of *PEPCK* and *G6Pase* were about twofold higher in B6 mice under fasting conditions when B6 mice were hypoinsulinemic relative to BTBR and F1 mice (Fig. 4, *B* and *C*). However, following insulin infusion, expression levels of *PEPCK* and *G6Pase* were reduced in B6 mice and no longer significantly different from BTBR and F1 mice (Figs. 4, *B* and *C*). It is possible that the reduction of glucose output was a result of a change in the activity of these enzymes. Thus, the levels of expression of these two insulin-responsive genes support the conclusion that there are no strain differences in hepatic insulin sensitivity.

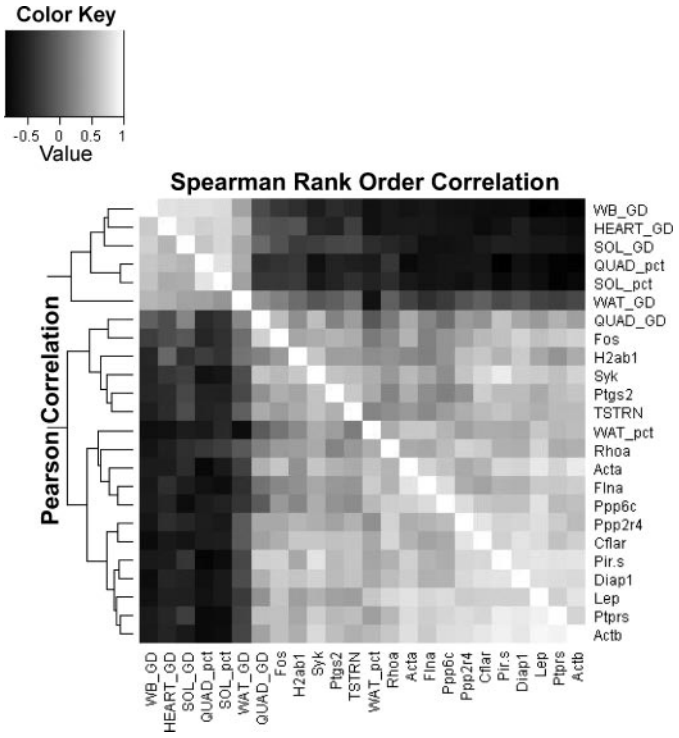

Fig. 3. Heat plot of the correlation matrix generated for whole body glucose disposal (WB-GD), heart-GD, soleus (SOL-GD), quadriceps (QUAD-GD), adipose (WAT-GD), quadriceps percentage (QUAD-ct), SOL-pct, WAT-pct, and adipose tissue mRNA expression. Cytoskeletal genes: β- and α-actin (Actb, Acta), diaphanous homolog-1 (Diap1), ras homolog gene family, member A (Rhoa), and filamin (Flna). Inflammatory genes: CASP8 and FADD-like apoptosis regulator (Cflar), FBJ osteosarcoma oncogene (Fos), histocompatibility 2, class II antigen A, β1 (H2ab1), paired immunoglobulin-like receptors (Pir.s: Pira6 isoforms and Lilrb/Pirb), prostaglandin-endoperoxide synthase-2 (Ptgs2/Cox-2), and spleen tyrosine kinase (Syk). Phosphatases: protein phosphatase 2A, regulatory subunit B (Ppp2r4), protein phosphatase 6, catalytic subunit (Ppp6c), and protein tyrosine phosphatase, receptor type, S (Ptprs). *Left*: Pearson correlations, which are in good agreement with Spearman rank order correlations illustrated on *right*. Data were organized by hierarchical clustering. White represents relationships with high positive correlation; black indicates high negative correlation.

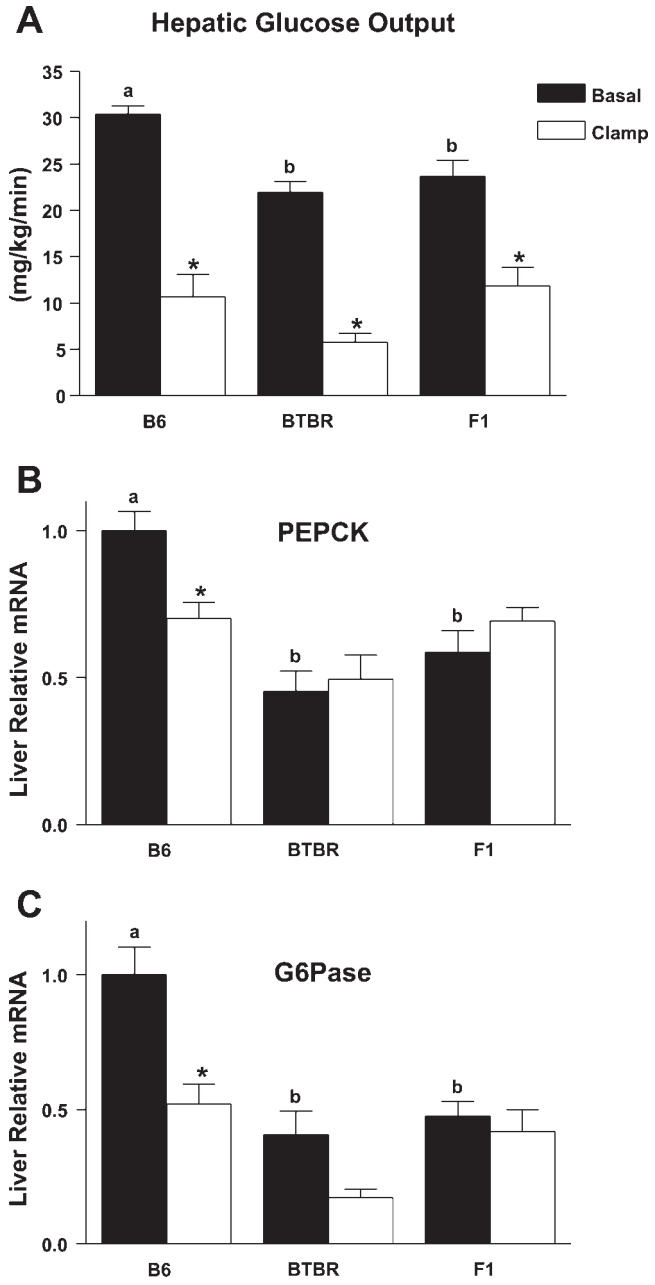

Fig. 4. Hepatic insulin sensitivity. *A*: basal hepatic glucose output (HGO) was determined by [3-^{3}H]glucose infusion under fasting (basal, filled bars) or hyperinsulinemic (2.5 mU·kg^{-1}·min^{-1}) conditions (clamp, open bars). *B*: hepatic phospho*enol*pyruvate carboxykinase (PEPCK) mRNA gene expression. *C*: hepatic glucose-6-phosphatase (G-6-Pase) expression. Values were normalized to β-actin and are expressed relative to B6 basal animals. Data represent means ± SE of 6–8 mice per group. Different letters designate a statistically significant difference by one-way ANOVA with Tukey's post test; *significant difference between basal and clamp measurements, $P < 0.05$.

DISCUSSION

Obesity and associated insulin resistance are a growing worldwide epidemic. The mechanisms regulating fat localiza-

Table 3. *Metabolic parameters in basal and clamp mice*

	B6	BTBR	F1
Plasma glucose, mg/dl			
Basal	221±11*	145±14*	193±10*
Clamp	108±1	105±5	111±8
Plasma insulin, ng/ml			
Basal	0.21±0.05*	0.91±0.15†	0.99±0.17†
Clamp	0.63±0.08*	1.49±0.33†	1.51±0.24†

Values are means ± SE of 6–8 mice per group. Different symbols designate a statistically significant difference by one-way ANOVA with Tukey's post test. Glucose values are the average of the last 3 time points (basal) and last 4 time points (clamp). Insulin values were obtained from plasma following heart puncture.

tion and pathogenicity remain poorly understood. Inbred mouse strains replicate much of the human genetic and sex variation in adiposity and insulin sensitivity. We studied two mouse strains, B6 and BTBR, which vary greatly in their level of abdominal obesity and fasting insulin levels. To determine the interplay among tissues contributing to insulin resistance in our model, we performed hyperinsulinemic euglycemic clamp experiments. We determined that BTBR and F1 mice exhibit insulin resistance primarily in heart, soleus muscle, and adipose tissue.

The finding of insulin resistance in BTBR soleus muscle is novel; previous in vitro studies did not identify a defect in this tissue. Muscle is the major site of insulin stimulated glucose disposal. Yet mice with selective loss of the insulin receptor in muscle (MIRKO) do not develop hyperglycemia (44). MIRKO mice have a compensatory increase in glucose uptake into adipose tissue, resulting in increased fat mass. In the present study, we observed insulin resistance in muscle without a compensatory increase in adipose tissue glucose uptake, suggesting that the obesity phenotype we observed is not a consequence of adipose tissue compensation for muscle insulin resistance. Furthermore, BTBR mice exhibit insulin resistance in isolated adipocytes, whereas muscle insulin resistance was observed only in vivo, suggesting that muscle changes might be secondary to the changes in adipose tissue.

BTBR mice exhibit differences in adipocyte insulin sensitivity in vitro (12). Fat replacement studies in adipose tissue-deficient mice revealed that adipose tissue is an important endocrine organ and not merely a storage site for excess energy (14). Reduced muscle glucose uptake was observed only in vivo and not in isolated muscle strips, suggesting that insulin-resistant adipose tissue produces a circulating factor capable of inhibiting muscle glucose uptake. Adipokines secreted from adipose tissue can either enhance (leptin, adiponectin) or impair (resistin, TNF-α, retinol-binding protein-4) insulin action in adipocytes, muscle, and liver (9, 15, 37, 55, 72, 84). Insulin resistance originating in adipose tissue may eventually affect all insulin target tissues, as was found in mice with adipose tissue-specific deficiency of the GLUT4 glucose transporter (1).

Much like the mice with loss of GLUT4 in adipose tissue, BTBR mice only exhibit muscle insulin resistance in vivo. This result is consistent with muscle insulin resistance being secondary to changes in adipose tissue. To investigate the role of adipose tissue in promoting systemic insulin resistance, we examined strain differences in adipose tissue gene expression. Consistent with the idea that obesity induces a state of inflammation (64, 80, 81, 83), the majority of the genes upregulated in BTBR and F1 mice are ones involved in inflammatory pathways. Higher leptin mRNA levels in BTBR and F1 adipose tissue suggest that their adipocytes are larger than those of B6 mice (20, 50). Hypertrophied adipocytes attract macrophages that secrete inflammatory molecules (80, 83). TNF-α is one such inflammatory molecule; it is capable of inhibiting insulin signaling in muscle, fat, and liver, resulting in hyperinsulinemia and hyperglycemia (55).

In addition to adipokines, estrogens and androgens may mediate changes in insulin sensitivity and inflammation (4, 13). Testosterone can inhibit secretion of adiponectin, an insulin-sensitizing molecule secreted from adipose tissue (82). Indeed, elevations in testosterone in BTBR and F1 mice are negatively correlated with whole body glucose disposal ($R = -0.493$, $P < 0.05$). Testosterone directly stimulates TNF-α production in macrophages (4). This finding provides a possible explanation for the pleotrophic effects mediated by testosterone: inflammatory responses and alterations in insulin sensitivity.

TNF-α was originally named cachectin, as it was found to induce cachexia (7), a wasting syndrome associated with severe trauma, infection, and cancer. Whereas cachexia is a severe pathological state, milder forms of wasting may be associated with obesity and insulin resistance. The low-grade chronic inflammation associated with increased adiposity may affect muscle protein synthesis or catabolism (11, 48). This provides a possible mechanism for the reduced muscle mass seen in BTBR and F1 mice. Indeed, we saw significant negative correlations between adipose inflammatory gene expression and muscle mass. Thus, reduced glucose disposal may be caused by inflammatory molecules inducing insulin resistance and reducing relative muscle mass. Therefore, targeting inflammation early and adding exercise or strength training to preserve muscle mass and function in prediabetes may be of critical importance in preventing progression to type 2 diabetes.

In summary, we determined that several inflammatory genes are induced in adipose tissue from insulin-resistant male mice. Consistent with the idea that inflammatory factors secreted from adipose tissue induce systemic insulin resistance, we found an association between inflammatory gene expression changes in adipose tissue and glucose uptake in heart and soleus muscle. Additionally, expression of inflammatory genes in adipose tissue negatively correlated with muscle mass. Elevations in testosterone in BTBR and F1 mice appear related to the pathological changes in adipose tissue and systemic insulin resistance. Further characterization of the insulin resistance in BTBR and F1 lean mice revealed that, despite significant peripheral insulin resistance, these mice maintain hepatic insulin sensitivity. Most adipokines, including TNF-α and adiponectin, affect hepatic glucose output (15, 46). Hence, it was surprising to find intact hepatic insulin sensitivity in BTBR and F1 mice. Further studies of BTBR and F1 mice may reveal important factors capable of preserving hepatic insulin sensitivity in individuals with obesity and insulin resistance.

ACKNOWLEDGMENTS

We thank Mary Rabaglia, Susanne Clee, and Hong Lan for technical assistance and intellectual contributions. We thank members of Gerald Schulman's lab for help with experimental design and members of Derry Roopenian's lab for help with RT-PCR primer design. We also thank Scott Hubbard-Van Stelle at the University of Wisconsin–Madison Research Animal Resources Center and various members of Denise M. Ney's lab for guidance on surgical techniques.

GRANTS

This work was supported by National Institute of Diabetes and Digestive and Kidney Diseases Grants DK-58037 and DK-66369. J. Flowers was supported by the Nutritional Sciences Departmental Predoctoral Training Grant DK-07665-11.

REFERENCES

1. **Abel ED, Peroni O, Kim JK, Kim YB, Boss O, Hadro E, Minnemann T, Shulman GI, Kahn BB.** Adipose-selective targeting of the GLUT4 gene impairs insulin action in muscle and liver. *Nature* 409: 729–733, 2001.
2. **Alberti KG, Zimmet PZ.** Definition, diagnosis and classification of diabetes mellitus and its complications. Part 1: diagnosis and classification of diabetes mellitus provisional report of a WHO consultation. *Diabet Med* 15: 539–553, 1998.
3. **American Diabetes Association.** Total prevalence of diabetes and prediabetes [Online]. Wick Davis. http://www.diabetes.org [7 July, 2006].
4. **Ashcroft GS, Mills SJ.** Androgen receptor-mediated inhibition of cutaneous wound healing. *J Clin Invest* 110: 615–624, 2002.
5. **Barbieri RL, Makris A, Randall RW, Daniels G, Kistner RW, Ryan KJ.** Insulin stimulates androgen accumulation in incubations of ovarian stroma obtained from women with hyperandrogenism. *J Clin Endocrinol Metab* 62: 904–910, 1986.
6. **Betuing S, Daviaud D, Valet P, Bouloumie A, Lafontan M, Saulnier-Blache JS.** Alpha2-adrenoceptor stimulation promotes actin polymerization and focal adhesion in 3T3F442A and BFC-1beta preadipocytes. *Endocrinology* 137: 5220–5229, 1996.
7. **Beutler B, Greenwald D, Hulmes JD, Chang M, Pan YC, Mathison J, Ulevitch R, Cerami A.** Identity of tumour necrosis factor and the macrophage-secreted factor cachectin. *Nature* 316: 552–554, 1985.
8. **Bogardus C, Lillioja S, Howard BV, Reaven G, Mott D.** Relationships between insulin secretion, insulin action, and fasting plasma glucose concentration in nondiabetic and noninsulin-dependent diabetic subjects. *J Clin Invest* 74: 1238–1246, 1984.
9. **Burcelin R, Kamohara S, Li J, Tannenbaum GS, Charron MJ, Friedman JM.** Acute intravenous leptin infusion increases glucose turnover but not skeletal muscle glucose uptake in ob/ob mice. *Diabetes* 48: 1264–1269, 1999.
10. **Chabowski A, Chatham JC, Tandon NN, Calles-Escandon J, Glatz J, Luiken JJ, Bonen A.** Fatty acid transport and Fat/Cd36 are increased in red but not in white skeletal muscle of Zucker diabetic fatty (ZDF) rats. *Am J Physiol Endocrinol Metab* 291: E675–E682, 2006.
11. **Charters Y, Grimble RF.** Effect of recombinant human tumour necrosis factor alpha on protein synthesis in liver, skeletal muscle and skin of rats. *Biochem J* 258: 493–497, 1989.
12. **Clee SM, Nadler ST, Attie AD.** Genetic and genomic studies of the BTBR ob/ob mouse model of type 2 diabetes. *Am J Ther* 12: 491–498, 2005.
13. **Clegg DJ, Brown LM, Woods SC, Benoit SC.** Gonadal hormones determine sensitivity to central leptin and insulin. *Diabetes* 55: 978–987, 2006.
14. **Colombo C, Cutson JJ, Yamauchi T, Vinson C, Kadowaki T, Gavrilova O, Reitman ML.** Transplantation of adipose tissue lacking leptin is unable to reverse the metabolic abnormalities associated with lipoatrophy. *Diabetes* 51: 2727–2733, 2002.
15. **Combs TP, Berg AH, Obici S, Scherer PE, Rossetti L.** Endogenous glucose production is inhibited by the adipose-derived protein Acrp30. *J Clin Invest* 108: 1875–1881, 2001.
16. **Coviello AD, Legro RS, Dunaif A.** Adolescent girls with polycystic ovary syndrome have an increased risk of the metabolic syndrome associated with increasing androgen levels independent of obesity and insulin resistance. *J Clin Endocrinol Metab* 91: 492–497, 2006.
17. **Dvorak RV, DeNino WF, Ades PA, Poehlman ET.** Phenotypic characteristics associated with insulin resistance in metabolically obese but normal-weight young women. *Diabetes* 48: 2210–2214, 1999.
18. **Einhorn D, Reaven GM, Cobin RH, Ford E, Ganda OP, Handelsman Y, Hellman R, Jellinger PS, Kendall D, Krauss RM, Neufeld ND, Petak SM, Rodbard HW, Seibel JA, Smith DA, Wilson PW.** American College of Endocrinology position statement on the insulin resistance syndrome. *Endocr Pract* 9: 237–252, 2003.
19. **Fagot-Campagna A, Narayan KM, Hanson RL, Imperatore G, Howard BV, Nelson RG, Pettitt DJ, Knowler WC.** Plasma lipoproteins and incidence of non-insulin-dependent diabetes mellitus in Pima Indians: protective effect of HDL cholesterol in women. *Atherosclerosis* 128: 113–119, 1997.
20. **Frederich RC, Lollmann B, Hamann A, Napolitano-Rosen A, Kahn BB, Lowell BB, Flier JS.** Expression of ob mRNA and its encoded protein in rodents. Impact of nutrition and obesity. *J Clin Invest* 96: 1658–1663, 1995.
21. **Freeman HC, Hugill A, Dear NT, Ashcroft FM, Cox RD.** Deletion of nicotinamide nucleotide transhydrogenase: a new quantitive trait locus accounting for glucose intolerance in C57BL/6J mice. *Diabetes* 55: 2153–2156, 2006.
22. **Friedman JE, de Vente JE, Peterson RG, Dohm GL.** Altered expression of muscle glucose transporter GLUT-4 in diabetic fatty Zucker rats (ZDF/Drt-fa). *Am J Physiol Endocrinol Metab* 261: E782–E788, 1991.
23. **Fujiwara T, Saitoh S, Takagi S, Takeuchi H, Isobe T, Chiba Y, Miura T, Shimamoto K.** Development and progression of atherosclerotic disease in relation to insulin resistance and hyperinsulinemia. *Hypertens Res* 28: 665–670, 2005.
24. **Gao S, Lee P, Wang H, Gerald W, Adler M, Zhang L, Wang YF, Wang Z.** The androgen receptor directly targets the cellular Fas/FasL-associated death domain protein-like inhibitory protein gene to promote the androgen-independent growth of prostate cancer cells. *Mol Endocrinol* 19: 1792–1802, 2005.
25. **Gilliver SC, Ashworth JJ, Mills SJ, Hardman MJ, Ashcroft GS.** Androgens modulate the inflammatory response during acute wound healing. *J Cell Sci* 119: 722–732, 2006.
26. **Goldfine AB, Bouche C, Parker RA, Kim C, Kerivan A, Soeldner JS, Martin BC, Warram JH, Kahn CR.** Insulin resistance is a poor predictor of type 2 diabetes in individuals with no family history of disease. *Proc Natl Acad Sci USA* 100: 2724–2729, 2003.
27. **Guilherme A, Emoto M, Buxton JM, Bose S, Sabini R, Theurkauf WE, Leszyk J, Czech MP.** Perinuclear localization and insulin responsiveness of GLUT4 requires cytoskeletal integrity in 3T3-L1 adipocytes. *J Biol Chem* 275: 38151–38159, 2000.
28. **Gulli G, Ferrannini E, Stern M, Haffner S, DeFronzo RA.** The metabolic profile of NIDDM is fully established in glucose-tolerant offspring of two Mexican-American NIDDM parents. *Diabetes* 41: 1575–1586, 1992.
29. **Haffner SM, Mykkanen L, Festa A, Burke JP, Stern MP.** Insulin-resistant prediabetic subjects have more atherogenic risk factors than insulin-sensitive prediabetic subjects: implications for preventing coronary heart disease during the prediabetic state. *Circulation* 101: 975–980, 2000.
30. **Haffner SM, Stern MP, Hazuda HP, Mitchell BD, Patterson JK.** Cardiovascular risk factors in confirmed prediabetic individuals. Does the clock for coronary heart disease start ticking before the onset of clinical diabetes? *JAMA* 263: 2893–2898, 1990.
31. **Haffner SM, Stern MP, Hazuda HP, Mitchell BD, Patterson JK.** Increased insulin concentrations in nondiabetic offspring of diabetic parents. *N Engl J Med* 319: 1297–1301, 1988.
32. **He J, Kelley DE.** Muscle glycogen content in type 2 diabetes mellitus. *Am J Physiol Endocrinol Metab* 287: E1002–E1007, 2004.
33. **Hegarty BD, Cooney GJ, Kraegen EW, Furler SM.** Increased efficiency of fatty acid uptake contributes to lipid accumulation in skeletal muscle of high fat-fed insulin-resistant rats. *Diabetes* 51: 1477–1484, 2002.
34. **Hirayama I, Yi Z, Izumi S, Arai I, Suzuki W, Nagamachi Y, Kuwano H, Takeuchi T, Izumi T.** Genetic analysis of obese diabetes in the TSOD mouse. *Diabetes* 48: 1183–1191, 1999.
35. **Hotamisligil GS, Murray DL, Choy LN, Spiegelman BM.** Tumor necrosis factor alpha inhibits signaling from the insulin receptor. *Proc Natl Acad Sci USA* 91: 4854–4858, 1994.
36. **Hotamisligil GS, Shargill NS, Spiegelman BM.** Adipose expression of tumor necrosis factor-alpha: direct role in obesity-linked insulin resistance. *Science* 259: 87–91, 1993.
37. **Hotamisligil GS, Spiegelman BM.** Tumor necrosis factor alpha: a key component of the obesity-diabetes link. *Diabetes* 43: 1271–1278, 1994.
38. **Hu FB.** The impact of diabetes and prediabetes on risk of cardiovascular disease and mortality. *Drugs Today (Barc)* 38: 769–775, 2002.
39. **Hu FB, Stampfer MJ, Haffner SM, Solomon CG, Willett WC, Manson JE.** Elevated risk of cardiovascular disease prior to clinical diagnosis of type 2 diabetes. *Diabetes Care* 25: 1129–1134, 2002.
40. **Irizarry RA, Hobbs B, Collin F, Beazer-Barclay YD, Antonellis KJ, Scherf U, Speed TP.** Exploration, normalization, and summaries of high density oligonucleotide array probe level data. *Biostatistics* 4: 249–264, 2003.

41. **Kapoor D, Malkin CJ, Channer KS, Jones TH.** Androgens, insulin resistance and vascular disease in men. *Clin Endocrinol (Oxf)* 63: 239–250, 2005.
42. **Karelis AD, St-Pierre DH, Conus F, Rabasa-Lhoret R, Poehlman ET.** Metabolic and body composition factors in subgroups of obesity: What do we know? *J Clin Endocrinol Metab* 89: 2569–2575, 2004.
43. **Kendziorski CM, Newton MA, Lan H, Gould MN.** On parametric empirical Bayes methods for comparing multiple groups using replicated gene expression profiles. *Stat Med* 22: 3899–3914, 2003.
44. **Kim JK, Michael MD, Previs SF, Peroni OD, Mauvais-Jarvis F, Neschen S, Kahn BB, Kahn CR, Shulman GI.** Redistribution of substrates to adipose tissue promotes obesity in mice with selective insulin resistance in muscle. *J Clin Invest* 105: 1791–1797, 2000.
45. **Kim JK, Zisman A, Fillmore JJ, Peroni OD, Kotani K, Perret P, Zong H, Dong J, Kahn CR, Kahn BB, Shulman GI.** Glucose toxicity and the development of diabetes in mice with muscle-specific inactivation of GLUT4. *J Clin Invest* 108: 153–160, 2001.
46. **Lang CH, Dobrescu C, Bagby GJ.** Tumor necrosis factor impairs insulin action on peripheral glucose disposal and hepatic glucose output. *Endocrinology* 130: 43–52, 1992.
47. **Leiter EH, Reifsnyder PC, Flurkey K, Partke HJ, Junger E, Herberg L.** NIDDM genes in mice: deleterious synergism by both parental genomes contributes to diabetogenic thresholds. *Diabetes* 47: 1287–1295, 1998.
48. **Li YP, Reid MB.** NF-κB mediates the protein loss induced by TNF-α in differentiated skeletal muscle myotubes. *Am J Physiol Regul Integr Comp Physiol* 279: R1165–R1170, 2000.
49. **Lillioja S, Mott DM, Spraul M, Ferraro R, Foley JE, Ravussin E, Knowler WC, Bennett PH, Bogardus C.** Insulin resistance and insulin secretory dysfunction as precursors of non-insulin-dependent diabetes mellitus. Prospective studies of Pima Indians. *N Engl J Med* 329: 1988–1992, 1993.
50. **Maffei M, Fei H, Lee GH, Dani C, Leroy P, Zhang Y, Proenca R, Negrel R, Ailhaud G, Friedman JM.** Increased expression in adipocytes of ob RNA in mice with lesions of the hypothalamus and with mutations at the db locus. *Proc Natl Acad Sci USA* 92: 6957–6960, 1995.
51. **Man ZW, Zhu M, Noma Y, Toide K, Sato T, Asahi Y, Hirashima T, Mori S, Kawano K, Mizuno A, Sano T, Shima K.** Impaired beta-cell function and deposition of fat droplets in the pancreas as a consequence of hypertriglyceridemia in OLETF rat, a model of spontaneous NIDDM. *Diabetes* 46: 1718–1724, 1997.
52. **McPhillips JB, Barrett-Connor E, Wingard DL.** Cardiovascular disease risk factors prior to the diagnosis of impaired glucose tolerance and non-insulin-dependent diabetes mellitus in a community of older adults. *Am J Epidemiol* 131: 443–453, 1990.
53. **Medalie JH, Papier CM, Goldbourt U, Herman JB.** Major factors in the development of diabetes mellitus in 10,000 men. *Arch Intern Med* 135: 811–817, 1975.
54. **Minokoshi Y, Kahn CR, Kahn BB.** Tissue-specific ablation of the GLUT4 glucose transporter or the insulin receptor challenges assumptions about insulin action and glucose homeostasis. *J Biol Chem* 278: 33609–33612, 2003.
55. **Muoio DM, Dohm GL, Fiedorek FT Jr, Tapscott EB, Coleman RA.** Leptin directly alters lipid partitioning in skeletal muscle. *Diabetes* 46: 1360–1363, 1997.
56. **Mykkanen L, Kuusisto J, Pyorala K, Laakso M.** Cardiovascular disease risk factors as predictors of type 2 (non-insulin-dependent) diabetes mellitus in elderly subjects. *Diabetologia* 36: 553–559, 1993.
57. **Nadler ST, Stoehr JP, Rabaglia ME, Schueler KL, Birnbaum MJ, Attie AD.** Normal Akt/PKB with reduced PI3K activation in insulin-resistant mice. *Am J Physiol Endocrinol Metab* 281: E1249–E1254, 2001.
58. **Nadler ST, Stoehr JP, Schueler KL, Tanimoto G, Yandell BS, Attie AD.** The expression of adipogenic genes is decreased in obesity and diabetes mellitus. *Proc Natl Acad Sci USA* 97: 11371–11376, 2000.
59. **Newton MA, Kendziorski CM, Richmond CS, Blattner FR, Tsui KW.** On differential variability of expression ratios: improving statistical inference about gene expression changes from microarray data. *J Comput Biol* 8: 37–52, 2001.
60. **Park KS, Rhee BD, Lee KU, Kim SY, Lee HK, Koh CS, Min HK.** Intra-abdominal fat is associated with decreased insulin sensitivity in healthy young men. *Metabolism* 40: 600–603, 1991.
61. **Pasquali R.** Obesity and androgens: facts and perspectives. *Fertil Steril* 85: 1319–1340, 2006.
62. **Perreault M, Marette A.** Targeted disruption of inducible nitric oxide synthase protects against obesity-linked insulin resistance in muscle. *Nat Med* 7: 1138–1143, 2001.
63. **Polonsky KS, Sturis J, Bell GI.** Seminars in Medicine of the Beth Israel Hospital, Boston. Non-insulin-dependent diabetes mellitus—a genetically programmed failure of the beta cell to compensate for insulin resistance. *N Engl J Med* 334: 777–783, 1996.
64. **Rajala MW, Scherer PE.** Minireview: The adipocyte—at the crossroads of energy homeostasis, inflammation, and atherosclerosis. *Endocrinology* 144: 3765–3773, 2003.
65. **Ranheim T, Dumke C, Schueler KL, Cartee GD, Attie AD.** Interaction between BTBR and C57BL/6J genomes produces an insulin resistance syndrome in (BTBR × C57BL/6J) F1 mice. *Arterioscler Thromb Vasc Biol* 17: 3286–3293, 1997.
66. **Rossetti L, Giaccari A.** Relative contribution of glycogen synthesis and glycolysis to insulin-mediated glucose uptake. A dose-response euglycemic clamp study in normal and diabetic rats. *J Clin Invest* 85: 1785–1792, 1990.
67. **Ruderman N, Chisholm D, Pi-Sunyer X, Schneider S.** The metabolically obese, normal-weight individual revisited. *Diabetes* 47: 699–713, 1998.
68. **Schwartz MA, Schaller MD, Ginsberg MH.** Integrins: emerging paradigms of signal transduction. *Annu Rev Cell Dev Biol* 11: 549–599, 1995.
69. **Sharma AM.** Adipose tissue: a mediator of cardiovascular risk. *Int J Obes Relat Metab Disord* 26, *Suppl* 4: S5–S7, 2002.
70. **Spiegelman BM, Farmer SR.** Decreases in tubulin and actin gene expression prior to morphological differentiation of 3T3 adipocytes. *Cell* 29: 53–60, 1982.
71. **Spiegelman BM, Ginty CA.** Fibronectin modulation of cell shape and lipogenic gene expression in 3T3-adipocytes. *Cell* 35: 657–666, 1983.
72. **Steppan CM, Bailey ST, Bhat S, Brown EJ, Banerjee RR, Wright CM, Patel HR, Ahima RS, Lazar MA.** The hormone resistin links obesity to diabetes. *Nature* 409: 307–312, 2001.
73. **Stoehr JP, Nadler ST, Schueler KL, Rabaglia ME, Yandell BS, Metz SA, Attie AD.** Genetic obesity unmasks nonlinear interactions between murine type 2 diabetes susceptibility loci. *Diabetes* 49: 1946–1954, 2000.
74. **Taylor SI.** Deconstructing type 2 diabetes. *Cell* 97: 9–12, 1999.
75. **Team RDC.** *R: A Language and Environment for Statistical Computing*. Vienna, Austria: R Foundation for Statistical Computing, 2005.
76. **Toye AA, Lippiat JD, Proks P, Shimomura K, Bentley L, Hugill A, Mijat V, Goldsworthy M, Moir L, Haynes A, Quarterman J, Freeman HC, Ashcroft FM, Cox RD.** A genetic and physiological study of impaired glucose homeostasis control in C57BL/6J mice. *Diabetologia* 48: 675–686, 2005.
77. **Tsakiridis T, Tong P, Matthews B, Tsiani E, Bilan PJ, Klip A, Downey GP.** Role of the actin cytoskeleton in insulin action. *Microsc Res Tech* 47: 79–92, 1999.
78. **Uysal KT, Wiesbrock SM, Marino MW, Hotamisligil GS.** Protection from obesity-induced insulin resistance in mice lacking TNF-alpha function. *Nature* 389: 610–614, 1997.
79. **von Eyben FE, Mouritsen E, Holm J, Montvilas P, Dimcevski G, Suciu G, Helleberg I, Kristensen L, von Eyben R.** Intra-abdominal obesity and metabolic risk factors: a study of young adults. *Int J Obes Relat Metab Disord* 27: 941–949, 2003.
80. **Weisberg SP, McCann D, Desai M, Rosenbaum M, Leibel RL, Ferrante AW Jr.** Obesity is associated with macrophage accumulation in adipose tissue. *J Clin Invest* 112: 1796–1808, 2003.
81. **Wellen KE, Hotamisligil GS.** Obesity-induced inflammatory changes in adipose tissue. *J Clin Invest* 112: 1785–1788, 2003.
82. **Xu A, Chan KW, Hoo RL, Wang Y, Tan KC, Zhang J, Chen B, Lam MC, Tse C, Cooper GJ, Lam KS.** Testosterone selectively reduces the high molecular weight form of adiponectin by inhibiting its secretion from adipocytes. *J Biol Chem* 280: 18073–18080, 2005.
83. **Xu H, Barnes GT, Yang Q, Tan G, Yang D, Chou CJ, Sole J, Nichols A, Ross JS, Tartaglia LA, Chen H.** Chronic inflammation in fat plays a crucial role in the development of obesity-related insulin resistance. *J Clin Invest* 112: 1821–1830, 2003.
84. **Yang Q, Graham TE, Mody N, Preitner F, Peroni OD, Zabolotny JM, Kotani K, Quadro L, Kahn BB.** Serum retinol binding protein 4 contributes to insulin resistance in obesity and type 2 diabetes. *Nature* 436: 356–362, 2005.
85. **Zhang B, Kirov S, Snoddy J.** WebGestalt: an integrated system for exploring gene sets in various biological contexts. *Nucleic Acids Res* 33: W741–W748, 2005.